

# An Effective Approach To Protect Lithium Anode and Improve Cycle Performance for Li–S Batteries

Feng Wu,<sup>†,‡,||</sup> Ji Qian,<sup>†,||</sup> Renjie Chen,<sup>\*,†,‡</sup> Jun Lu,<sup>\*,§</sup> Li Li,<sup>†,‡</sup> Huiming Wu,<sup>§</sup> Junzheng Chen,<sup>†</sup> Teng Zhao,<sup>†</sup> Yusheng Ye,<sup>†</sup> and Khalil Amine<sup>\*,§</sup>

<sup>†</sup>Beijing Key Laboratory of Environmental Science and Engineering, School of Chemical Engineering and Environment, Beijing Institute of Technology, Beijing 100081, P.R. China

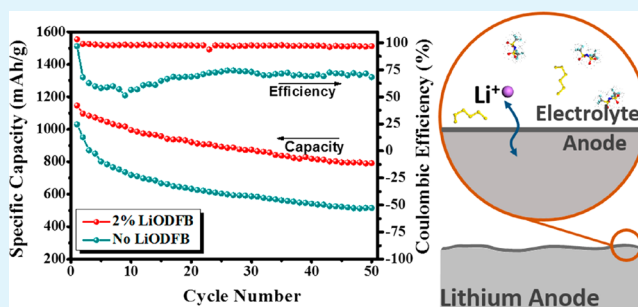
<sup>‡</sup>National Development Center of High Technology Green Materials, Beijing 100081, P.R. China

<sup>§</sup>Chemical Sciences and Engineering Division, Argonne National Laboratory, 9700 South Cass Avenue, Lemont, Illinois 60440, United States

## S Supporting Information

**ABSTRACT:** Lithium oxalyldifluoroborate (LiODFB) has been investigated as an organic electrolyte additive to improve the cycling performance of Li–S batteries. Cell test results demonstrate that an appropriate amount of LiODFB added into the electrolyte leads to a high Coulombic efficiency. Analyses by energy dispersive X-ray spectroscopy, X-ray photoelectron spectroscopy, and the density functional theory showed that LiODFB promotes the formation of a LiF-rich passivation layer on the lithium metal surface, which not only blocks the polysulfide shuttle, but also stabilizes the lithium surface.

**KEYWORDS:** lithium–sulfur batteries, lithium anode, electrolyte, LiODFB, passivation layer, electrochemistry



## INTRODUCTION

Rechargeable batteries with high energy density and long cycle life are in urgent demand for electric vehicles and other energy storage systems.<sup>1</sup> The Li–S battery is a promising electrochemical system because of its high theoretical specific capacity (1672 mAh/g) and energy density (2600 Wh/kg). In addition, the active material, sulfur, is low cost, highly abundant, and nontoxic, which makes the Li–S battery even more attractive. However, despite much development effort in the past years, Li–S batteries have not yet reached commercialization because of several technical bottlenecks.<sup>2–4</sup> One of the biggest challenges is the insulating nature of sulfur and its reduction products ( $\text{Li}_2\text{S}$  and  $\text{Li}_2\text{S}_2$ ), which result in low electronic conductivity within sulfur electrodes. Cathode materials that incorporate sulfur into a different carbon matrix,<sup>5–11</sup> or conductive polymers,<sup>12–14</sup> were developed to improve the electrical conductivity and accommodate the electrode volume expansion during cell operation. Another challenge is the solubility of the long-chain polysulfide ions generated during the charge and discharge of the cell, which gives rise to a “shuttle” mechanism. This shuttle effect not only decreases utilization of the active material, but also markedly reduces the Coulombic efficiency of the cell.<sup>15</sup> To overcome this problem, the cathode materials have been tuned to better encapsulate sulfur and thereby suppress the dissolution of polysulfides into the electrolyte; however, such cathode structures only provide limited success in solving the polysulfide dissolution problem.

Various researchers have investigated optimization of the electrolyte as a different avenue to tackle this problem. In particular, a pseudosolid-state electrolyte (the solvent-in-salt electrolyte<sup>16</sup> with an ultrahigh salt concentration) and an all-solid-state electrolyte<sup>17</sup> have been developed for Li–S cells, which demonstrate improved Coulombic efficiency and cycle stability because of the dramatic decrease in the solubility of the lithium polysulfides. However, the challenge facing solid-state electrolytes is the low ionic conductivity at room temperature, which has a significant impact on the rate performance of the cell. In addition, these electrolytes are usually very costly and difficult to fabricate at the current stage; therefore, organic liquid remains the electrolyte of choice for Li–S batteries. Nonetheless, as mentioned earlier, the shuttle effect from the polysulfide dissolution that occurs in pure organic liquid electrolytes is problematic. For that reason, electrolyte additives are commonly used to alleviate the shuttle problem. For instance,  $\text{LiNO}_3$  was widely used as the additive or cosalt in the electrolyte for Li–S cells because it helps to protect the lithium electrode by forming a surface protective film.<sup>18–20</sup> This film can effectively suppress the redox shuttle reactions, and thus improves the cycle performance and Coulombic efficiency of the Li–S cell.<sup>18</sup> However,  $\text{LiNO}_3$  can be reduced on the

Received: July 4, 2014

Accepted: August 6, 2014

Published: August 6, 2014

cathode at potentials lower than 1.6 V, and the formed byproducts severely affect the reversibility of the sulfur cathode. The narrower voltage window of a cell containing  $\text{LiNO}_3$  in the electrolyte causes a loss of capacity.<sup>20,21</sup> A strong oxidant in the presence of acidity,  $\text{LiNO}_3$  will potentially increase the safety issues of the cell during long-term cycling if it is not consumed completely. Therefore, researchers are seeking alternative electrolyte additives that can reduce the shuttle effect in the Li–S cell.<sup>22,23</sup>

Lithium oxalyldifluoroborate (LiODFB) salt, which has a chemical structure that comprises the half molecular moieties of LiBOB and  $\text{LiBF}_4$ ,<sup>24</sup> has been reported to improve the electrochemical performance of Li-ion batteries. Since LiODFB exploits advantages of both LiBOB and  $\text{LiBF}_4$ , it possesses thermal stability, optimized ionic conductivity over a wide temperature range, and the ability to passivate Al at high potential.<sup>24–26</sup> In this work, we studied the effects of LiODFB as an electrolyte additive on the electrochemical performance of Li–S cells for the first time. The results demonstrate that the addition of an appropriate amount of LiODFB to the electrolyte promotes the formation of a surface passivation layer on the lithium electrode, which significantly suppresses the parasitic reactions between polysulfides and the lithium electrode and offers the promise of high Coulombic efficiency and a long cycle life for the Li–S battery.

## RESULTS AND DISCUSSION

To investigate the effect of the LiODFB additive on the electrochemical performance of the Li–S cell, we selected a

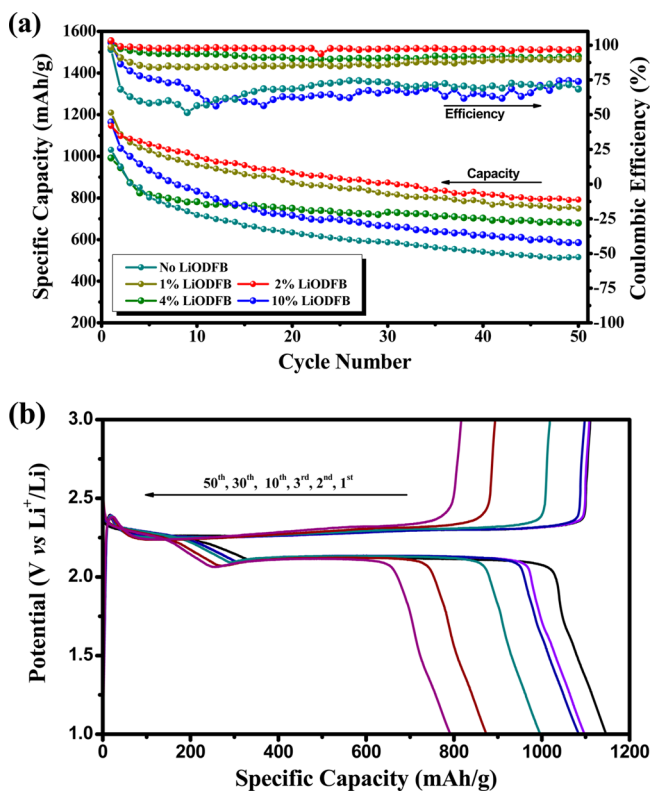


**Figure 1.** (a) Capacity versus cycle number for Li–S cells with different amounts of LiODFB added. (b) Discharge and charge curves of the cell with 2% LiODFB additive on different cycles. All of the electrochemical measurements were performed at a current of 100 mA/g-sulfur.

multiwalled carbon nanotube (MWCNT) with a sulfur composite as the cathode active material. The method for preparation of this cathode material can be found elsewhere.<sup>11,14</sup> The sulfur content in the cathode was confirmed (Figure S1 of the Supporting Information) by thermogravimetric analysis to be 67 wt %. The pure electrolyte used was 1.0 mol/L bis(trifluoromethane)sulfonimide lithium (LiTFSI) in dimethoxyethane (DME) and 1,3-dioxolane (DOL) (see the Experimental section).

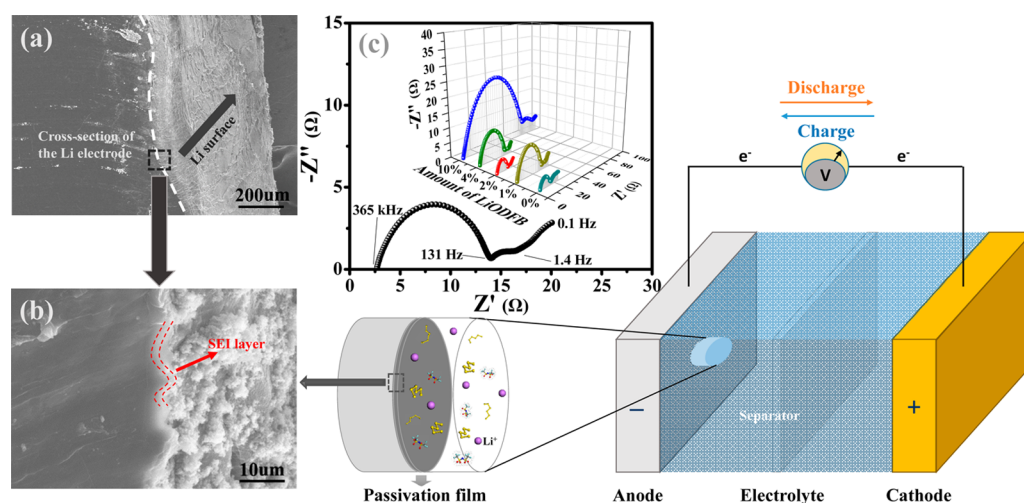
Figure 1a shows the specific capacities and Coulombic efficiencies as functions of cycle numbers for Li–S cells with different amounts of LiODFB added to the electrolyte (i.e., 0, 1%, 2%, 4%, and 10%, respectively). Clearly, the Li–S cell with no LiODFB shows poor electrochemical performance. The capacity undergoes a fast decay during the first 5 cycles, and the capacity retention of this cell is only 50% after 50 cycles. Meanwhile, the Coulombic efficiency of this cell drops sharply from 97% to below 70% in the first 2 cycles. This poor electrochemical performance is believed to be associated with the severe shuttle phenomenon. After different amounts of LiODFB were added to the electrolyte, both the capacity retention and Coulombic efficiency improved, as illustrated in Figure 1, panel (a). Interestingly, the cell with 2% LiODFB additive exhibited the best electrochemical performance. For this cell, the initial capacity (based on the mass of sulfur loading) was 1146.4 mAh/g, and the capacity retention after 50 cycles was about 70%. Moreover, the Coulombic efficiency improved dramatically and remained at 97% during the cycle test.

Figure 1, panel b shows the charge and discharge curves of the Li–S cell with 2% LiODFB additive. The discharge curves comprises two typical plateaus (2.3 V and 2.1 V vs  $\text{Li}^+/\text{Li}$ ), which correspond to the reduction of sulfur to soluble polysulfides and the further reduction of polysulfides to  $\text{Li}_2\text{S}_2/\text{Li}_2\text{S}$ , respectively. The multistep electrochemical reactions of elemental sulfur with lithium ions in these cells are further demonstrated by the cyclic voltammetry results in Figure S2 of the Supporting Information.

It is noteworthy that the cell performance decreases when the amount of LiODFB additive increases, as is evident by the low Coulombic efficiency of the cell with 10% LiODFB, which is similar to that of the cell with no LiODFB (Figure 1a). This result suggests that a fairly thick layer is formed on the lithium electrode for the cell with more than 2% LiODFB added, which likely blocks further ion transportation and thus leads to a low Coulombic efficiency. In other words, the adjustment of the amount of LiODFB added to the electrolyte is critical to tune the solid–electrolyte interphase (SEI) that forms on the lithium electrode.

The above results demonstrate that the addition of the appropriate amount of LiODFB into the electrolyte improves the electrochemical performance of the Li–S cell. We attribute this improvement to the formation of a protective layer on the lithium electrode to suppress the shuttle effect. The scanning electron microscopy (SEM) images of the cross-section of the lithium electrodes after the cycle test in the cell containing 2% LiODFB clearly show the formation of a dense passivation layer on the anode (Figures 2a,b).

To study the passivation layer on lithium electrodes, an AC impedance analysis of the cells after 50 cycles was performed over a frequency range of 100 mHz to 1 MHz. As shown in Figure 2, panel c, the spectra with the LiODFB added displays two semicircles, while that with no LiODFB added only has



**Figure 2.** Schematic configuration of the Li–S cell (on the right side). Scanning electron micrographs of the cross-section of the lithium electrode with 2% LiODFB after 50 cycles at (a) low and (b) high magnifications. (c) The alternating current (AC) impedance measurements of the lithium electrode with 2% LiODFB added into the electrolyte. The inset shows the AC impedance of the cells with different amounts of LiODFB added. All of the lithium electrodes measured were after 50 cycles.

one. As has been intensively studied,<sup>27–30</sup> the semicircle at high frequency is associated with the passivation surface film, which can be characterized by a parallel combination between the resistance ( $R_{\text{sei}}$ ) and capacitance ( $C_{\text{sei}}$ ) of the SEI on the surface of the electrode, while the semicircle at a medium frequency is related to charge-transfer processes and can be described on the basis of the parallel combination between the charge-transfer resistance ( $R_{\text{ct}}$ ) and the double-layer capacitance ( $C_{\text{dl}}$ ). Specifically, while no main electrochemical reactions take place, the  $R_{\text{ct}}$  is so high that its semicircle becomes invisible.<sup>28</sup> Roughly speaking, the passivation film resistance ( $R_{\text{sei}}$ ) increases with the LiODFB weight percent, but the  $R_{\text{sei}}$  is lowest with 2% LiODFB added. According to the results in other papers,<sup>18,22</sup> LiTFSI's contribution to the passivation film is negligible, and with no LiODFB, the main component of the SEI is  $\text{Li}_2\text{S}$ , which is a poor lithium-ion conductor, but in the case of LiODFB added, it participates in the formation of a passivation layer that contributes to Li-ion conduction. An increase in the amount of LiODFB added beyond 2 wt % may thicken the passivation film, delivering a larger  $R_{\text{sei}}$ . We thus believe that the low  $R_{\text{sei}}$  is a major factor behind the much improved electrochemical performance of the Li–S cell containing 2% LiODFB.

We used SEM to investigate the surface morphology of the lithium electrodes after 10 cycles with various amounts of LiODFB added. As seen in Figure S3b of the Supporting Information, the surface of the lithium electrode with no LiODFB became rough and loose after 10 cycles compared to the smooth and compact surface of the pristine lithium electrode (Figure S3a, Supporting Information). As previously reported,<sup>31,32</sup> the rough lithium surface has a higher specific surface area, which is detrimental to the performance of Li–S cells and may lead to some other safety problems such as cell swelling and thermal instability. Fortunately, adding LiODFB into the electrolyte for Li–S cells can help alleviate the problem. As shown in Figure S3 (Supporting Information), a smoother and denser surface morphology on the anode appears when the LiODFB additive was used. Furthermore, the roughness of the surface morphology decreases when the LiODFB weight percent increases. When we replaced the LiTFSI with LiODFB (1 mol/L) as the lithium electrolyte salt,

the lithium electrode exhibited a highly uniform and compact surface morphology (Figure S4, Supporting Information). In this way, the reactions of the lithium anode and electrolyte solvent or the dissolved polysulfides can be effectively controlled, which results in capacity fading and thermal instability.

Figure 3, panels a and b show the surface morphology of the lithium electrode after 50 cycles with no and 2% LiODFB added into the electrolyte, respectively. As shown, the surface morphology of the lithium electrode with no LiODFB became looser and rougher, while that with 2% LiODFB was relatively smooth, except for some cracks (as indicated by the rectangles in Figure 3b). Once a crack appears before cycling or on the initial cycle, the lithium in this area will exhibit relatively higher reactivity with the electrolyte, which leads to growth of the crack. This process is similar to the mechanism of dendrite formation in Li-ion batteries, and the rough surface morphology that occurs is harmful for batteries, as described previously.

As confirmed in other papers,<sup>16,18,22</sup> the improved cycling efficiency in the modified electrolyte system is related to the SEI formed on the surface of the lithium electrode. To determine the chemical composition of the passivation film, we performed energy dispersive X-ray (EDX) spectroscopy and X-ray photoelectron spectroscopy (XPS). The EDX results of the lithium electrode surface after 50 cycles with no and 2% LiODFB added are presented in Figure 3, panels c and d and in Table S1 of the Supporting Information. The fluorine elemental map (Figure 3c) proves that the surface is uniformly covered by the passivation film; however, some concentrated areas appear in the sulfur elemental map (marked by a white rectangle in Figure 3d) and correspond to the cracks in Figure 3, panel b. This finding demonstrates that a greater part of  $\text{Li}_2\text{S}_2/\text{Li}_2\text{S}$  was precipitated in these areas, which confirms the higher reactivity of the lithium in these areas. The EDX results listed in Table S1 (Supporting Information) show the maps of several elements (O, C, F, and S) on the lithium electrode surface. (Since oxygen and carbon might arise from the organic compounds in the electrolyte or the atmosphere within the glovebox used during cell assembly and operation, they will be ignored here.) The data in Table S1 of the Supporting

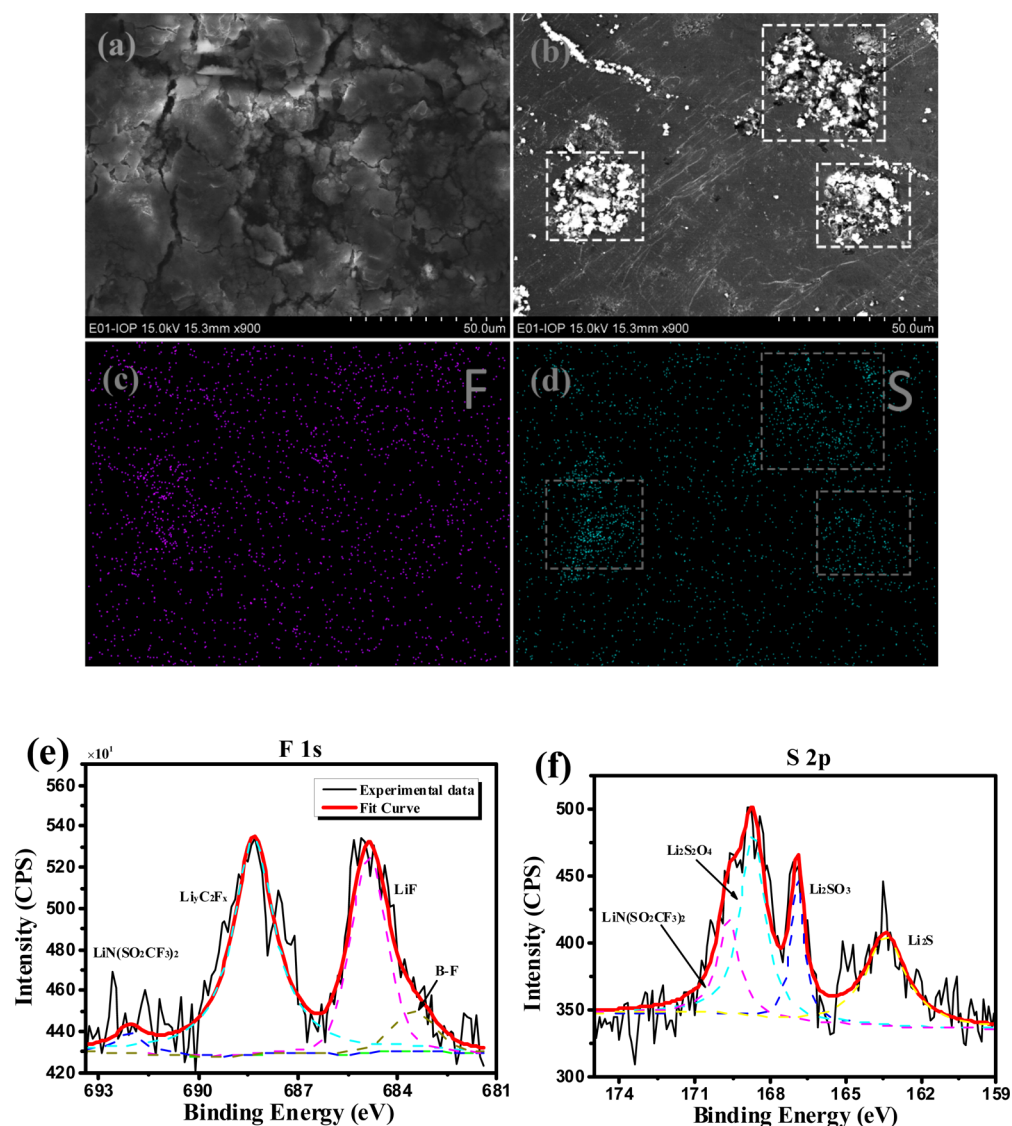
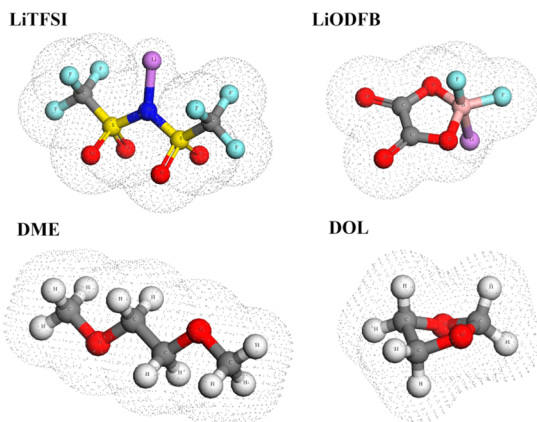


**Figure 3.** SEM images of the lithium electrodes after 50 cycles with (a) no LiODFB and (b) 2% LiODFB. (c,d) EDX mapping of the lithium electrode in panel b, which shows the distribution of fluorine and sulfur. (e,f) XPS spectra (F 1s; S 2p) of the lithium electrode surface with 2% LiODFB after 50 cycles.

### Scheme 1. Structures of the Lithium Salts and Organic Solvents Used

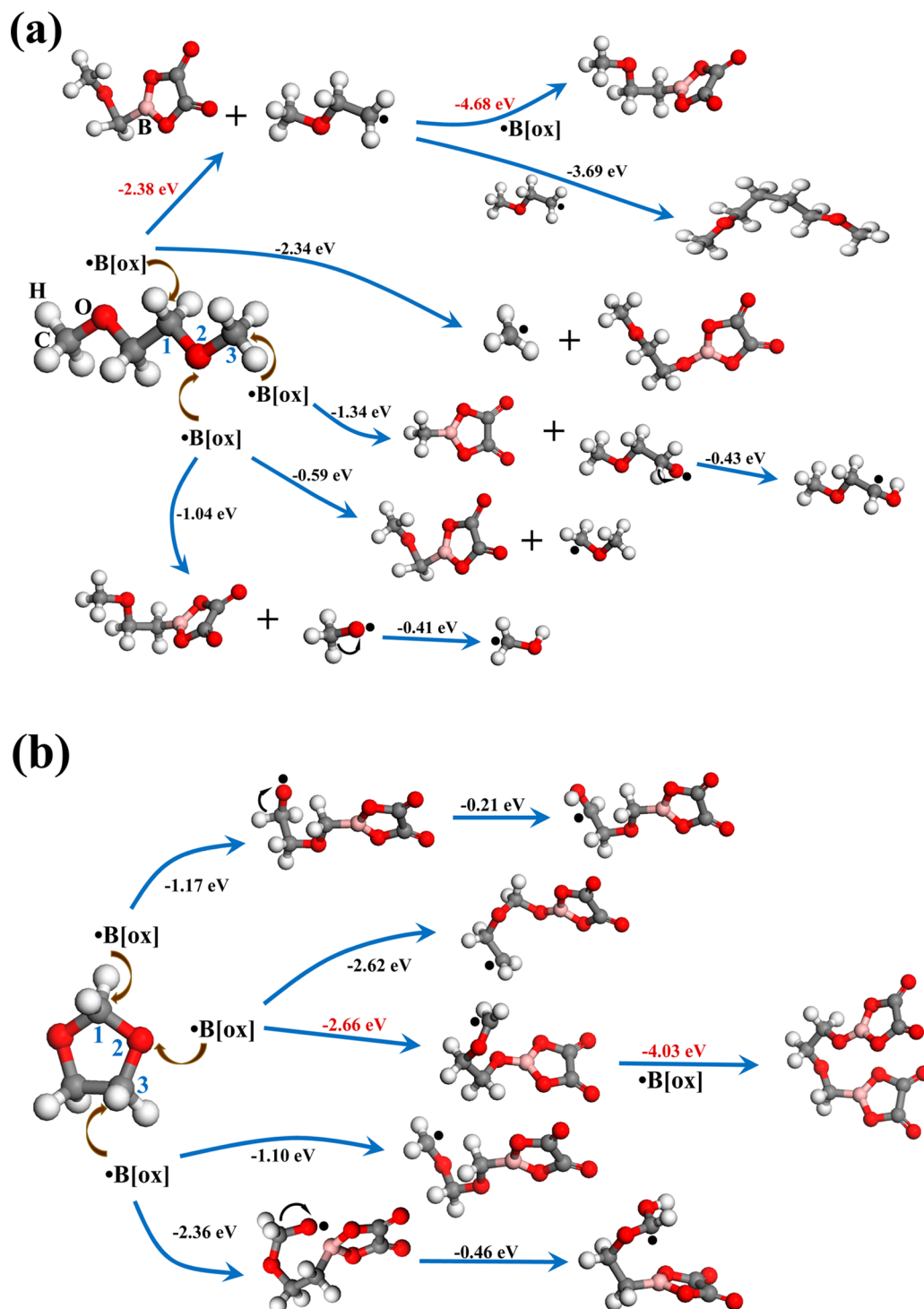


Information indicate that, after the addition of 2% LiODFB, the molar ratio of fluorine to sulfur on the surface of the lithium

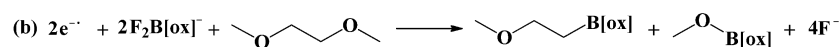
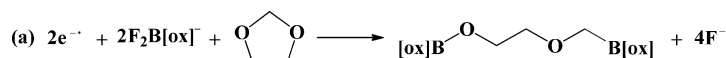
electrode increased from 2.17 to 6.93. This finding suggests that the fluorine-containing substance, namely LiODFB, is involved in the formation of the passivation layer, which can inhibit the reaction between lithium and the electrolyte and thus reduces the amount of  $\text{Li}_2\text{S}_2/\text{Li}_2\text{S}$  deposited on the surface of the lithium electrode.

Complementary information on the lithium electrode surfaces with 2% LiODFB was provided by the XPS analysis (Figures 3e,f and Figure S5 of the Supporting Information). According to the XPS data and previous work reported by other groups,<sup>16,18</sup> the main components of the SEI layer (2% LiODFB added) are similar to those of the SEI layer with no LiODFB, except for much more LiF and a trace of boron detected. It is worth noting that the Li–S cells with a fluorinated electrolyte show improved performance.<sup>33–35</sup> Also, HF can be generated through reactions within the electrolyte-containing  $\text{LiBF}_4$  in Li-ion batteries and simultaneously will react with the alkali components in the SEI layer to form  $\text{LiF}$ <sup>36</sup> and thus improves the morphology of the graphite electrode for lithium deposition.<sup>37</sup> Our experimental results indicate that

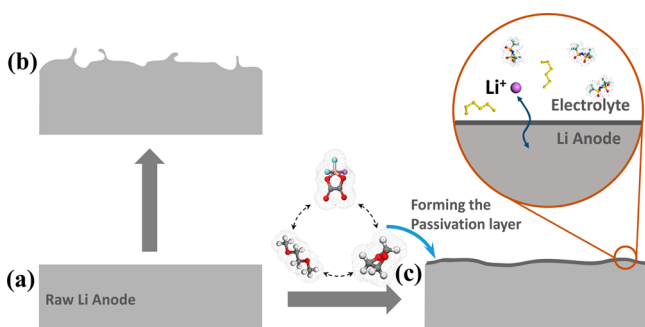
Scheme 2. Possible Reactions of the  $\bullet\text{B}[\text{ox}]$  Radical with (a) DME and (b) DOL, Where  $\bullet\text{B}[\text{ox}]$  Represents Oxalatoberylyl Radical, and the DFT Estimates for Enthalpies of Individual Reaction Steps at the Temperature of Absolute Zero are Given



Scheme 3. Proposed Reactions between LiODFB and DOL/DME, Where  $\text{F}_2\text{B}[\text{ox}]^-$  Represents the Oxalyldifluoro(oxalate)borate Anion



#### Scheme 4. Schematic Illustration of the Role of LiODFB in Forming the Passivation Layer<sup>a</sup>



<sup>a</sup>Lithium anode (a) before cycling and (b) after cycles with no LiODFB added. (c) Lithium anode after cycles with LiODFB additive, which promotes the formation of the passivation layer.

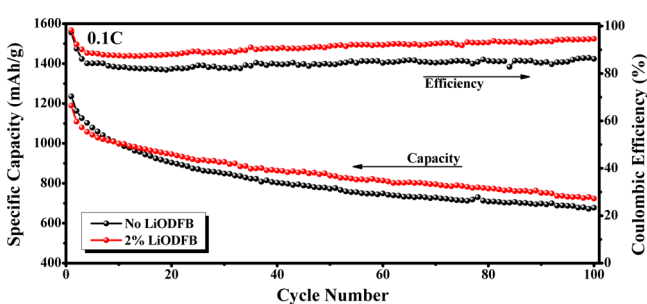


**Figure 4.** Comparison of the cycle performance between cells with no and 2% LiODFB added, where the cathode active material is GS-MWCNT@S composite. The electrochemical measurements were performed at a current of 0.1 C (1 C = 1675 mA/g-sulfur).

LiODFB helps stabilize the lithium surface through the reactions between LiODFB and other substances in this system during cycling, but the mechanism is not entirely clear. We thus performed *ab initio* simulations in the form of the density functional theory (DFT) to further study the mechanism.

The oxalyldifluoro(oxalate)borate anion ( $F_2B[ox]^-$ ) was reported to reduce at 1.6 V,<sup>38</sup> which corresponds to the cyclic voltammetry results (Figure S2, Supporting Information), and the reduction process is the stepwise elimination of  $F^-$  anions, which produces the oxalato-boryl radical ( $*B[ox]$ ).<sup>39</sup> The tentative oxalato-boryl radical may react with DME and DOL molecules (structures are shown in Scheme 1), and the DFT calculations of the individual reaction steps at the temperature of absolute zero are listed in Scheme 2. The reactions, which produce several chain hydrocarbons, are favored energetically (enthalpies of the individual reaction steps are marked in red in Scheme 2), and the proposed net reactions of the  $F_2B[ox]^-$  anion with DME and DOL are given in Scheme 3. The resulting terminal products might account for the benign role of LiODFB in SEI formation, but the process is not fully understood, and research into this mechanism is ongoing. Overall, LiODFB has the ability to facilitate SEI formation on the lithium electrode, which improves cell performance. A simplified process is shown in Scheme 4.

To verify the compatibility of the modified electrolyte with another sulfur composite cathode, we chose a graphene-based sulfur/MWCNT composite with 70 wt % sulfur (GS-MWCNT@S). Figure 4 shows the performance of the Li-S cells with no and 2% LiODFB operated for 100 cycles. In the case of 2% LiODFB, the Coulombic efficiency increased slowly

during cycling and reached a level of 94.6% after 100 cycles, which is obviously higher than that of the cell with no LiODFB. In addition, the cell with 2% LiODFB delivered an initial capacity of 1189.5 mAh/g. These results imply that the modified electrolyte with 2% LiODFB could be compatible with other sulfur composite cathodes for the Li-S cell and delivers a stable electrochemical performance. But it can be observed that the cell capacity drops still exist, so novel cathode materials, with the properties of high conductivity, favorable adsorption properties, and mechanically robust character, need to be developed.

## CONCLUSIONS

In summary, we investigated the effects of LiODFB as an electrolyte additive on the electrochemical properties of Li-S cells. The Li-S cells with the LiODFB-added electrolyte exhibited extremely high Coulombic efficiency and better cycle performance, and the experimental results demonstrate that the appropriate amount of LiODFB electrolyte additive is 2 wt %. The role of LiODFB in Li-S cells is to promote a LiF-rich passivation layer on the lithium anode surface. The passivation layer not only blocks the polysulfide shuttle mechanism, thus improving the electrochemical performance, but also stabilizes the lithium surface. In general, LiODFB is a promising electrolyte additive for Li-S batteries, but the mechanism is still not clear, and a deeper understanding and more detailed knowledge of it are needed.

## EXPERIMENTAL SECTION

**Synthesis.** The pure electrolyte used was 1.0 mol/L LiTFSI salt (3M) in a solvent of DME and DOL (volume ratio of 1:1, Alfa Aesar). Different amounts (1%, 2%, 4%, and 10%, by weight) of LiODFB (Hongyang Chemical, China) were added to the electrolyte. Structures of the lithium salts and organic solvents are illustrated in Scheme 1.

**Electrochemical Measurements.** A MWCNT/S composite was prepared by a simple melt-diffusion strategy. Then, cathode slurries were produced by mixing 70% MWCNT/S composite, 20% acetylene black, and 10% polyvinylidene fluoride binder in *N*-methyl-2-pyrrolidinone. The mixtures were ball milled for 4 h to form homogeneous slurries. After stirring, each slurry was coated onto aluminum foil using a roll press. The coated electrodes were dried in a vacuum oven at 60 °C for 24 h. The electrodes were cut into disks with a diameter of 11 mm. Two-electrode coin cells (CR2025) with Li foil as the anodes were assembled in an argon-filled glovebox for electrochemical experiments. The cells were discharged and charged between cutoff potentials of 1.0 and 3.0 V using an electrochemical station (LAND, Wuhan, China) to test their cycle life, where the current was 100 mA/g. Cyclic voltammograms were recorded on an electrochemical workstation (CHI660D, Shanghai Chenhua, China) between 1.0 and 3.0 V to characterize the redox behavior and kinetic reversibility of the cells.

**Characterizations and Computation.** Thermal gravimetric analysis (TGA) of the cathode material was carried out using a thermal analyzer (6200 EXSTAR) at a heating rate of 10 °C/min under an air atmosphere. The cells were unpacked in the glovebox after cycling, and the lithium electrodes were removed and then thoroughly washed with a large amount of DOL three times. The AC impedance of the lithium electrodes after 50 cycles was measured with an impedance analyzer (Zahner Zennium). The AC amplitude was  $\pm 5$  mV, and the applied frequency range was 100 mHz to 1 MHz. The morphology and composition of the surfaces of the lithium electrode surface were investigated with EDX and SEM (HTACHI S-4800). Also, XPS (ESCALAB 250) was performed using a monochromatized Al K $\alpha$  source. Geometry optimizations of the radicals were carried out with the all-electron density functional program DMol3 in Materials Studio 5.5 (Accelrys) using the Becke–Lee–Yang–Parr (BLYP)

functional and the double numerical plus polarization (DNP) basis set. The optimization was considered converged when the following convergence criteria were met:  $1.0 \times 10^{-5}$  Ha for the total energy, 0.002 Ha/Å for the maximum force on atoms, and 0.005 Å for the maximum atomic displacement.

## ■ ASSOCIATED CONTENT

### ■ Supporting Information

EDX results from the SEM images shown in this work. TGA curve of the MWCNT/S composite. Cyclic voltammograms of the Li–S cell. SEM images of the Li electrodes after 10 cycles. XPS spectra of the Li electrode surface. This material is available free of charge via the Internet at <http://pubs.acs.org>.

## ■ AUTHOR INFORMATION

### Corresponding Authors

\*E-mail: [chenrj@bit.edu.cn](mailto:chenrj@bit.edu.cn).

\*E-mail: [junlu@anl.gov](mailto:junlu@anl.gov).

\*E-mail: [amine@anl.gov](mailto:amine@anl.gov).

### Notes

The authors declare no competing financial interest.

<sup>†</sup>F.W. and J.Q. contributed equally to this work.

## ■ ACKNOWLEDGMENTS

This work was supported by the National Science Foundation of China (21373028), the National 863 Program (2011AA11A256), the New Century Educational Talents Plan of Chinese Education Ministry (NCET-12-0050), the Beijing Novel Program (Z121103002512029), and the Ford University Research Program (URP) project. This work was also supported by the U.S. Department of Energy under Contract No. DE-AC0206CH11357 from the Vehicle Technologies Office, Department of Energy, Office of Energy Efficiency and Renewable Energy (EERE). Argonne National Laboratory is operated for the U.S. Department of Energy by UChicago Argonne, LLC, under Contract No. DE-AC02-06CH11357.

## ■ REFERENCES

- (1) Armand, M.; Tarascon, J. M. Building Better Batteries. *Nature* **2008**, *451*, 652–657.
- (2) Ji, X.; Nazar, L. F. Advances in Li–S Batteries. *J. Mater. Chem.* **2010**, *20*, 9821–9826.
- (3) Bruce, P. G.; Freunberger, S. A.; Hardwick, L. J.; Tarascon, J. M. Li–O<sub>2</sub> and Li–S Batteries with High Energy Storage. *Nat. Mater.* **2012**, *11*, 19–29.
- (4) Manthiram, A.; Fu, Y.; Su, Y.-S. Challenges and Prospects of Lithium–Sulfur Batteries. *Acc. Chem. Res.* **2012**, *46*, 1125–1134.
- (5) Ji, X.; Lee, K. T.; Nazar, L. F. A Highly Ordered Nanostructured Carbon–Sulphur Cathode for Lithium–Sulphur Batteries. *Nat. Mater.* **2009**, *8*, 500–506.
- (6) Wang, H.; Yang, Y.; Liang, Y.; Robinson, J. T.; Li, Y.; Jackson, A.; Cui, Y.; Dai, H. Graphene-Wrapped Sulfur Particles as a Rechargeable Lithium–Sulfur Battery Cathode Material with High Capacity and Cycling Stability. *Nano Lett.* **2011**, *11*, 2644–2647.
- (7) Ji, L.; Rao, M.; Zheng, H.; Zhang, L.; Li, Y.; Duan, W.; Guo, J.; Cairns, E. J.; Zhang, Y. Graphene Oxide as a Sulfur Immobilizer in High Performance Lithium/Sulfur Cells. *J. Am. Chem. Soc.* **2011**, *133*, 18522–18525.
- (8) Jayaprakash, N.; Shen, J.; Moganty, S. S.; Corona, A.; Archer, L. A. Porous Hollow Carbon–Sulfur Composites for High-Power Lithium–Sulfur Batteries. *Angew. Chem., Int. Ed.* **2011**, *123*, 6026–6030.
- (9) Guo, J.; Xu, Y.; Wang, C. Sulfur-Impregnated Disordered Carbon Nanotubes Cathode for Lithium–Sulfur Batteries. *Nano Lett.* **2011**, *11*, 4288–4294.
- (10) Zheng, G.; Yang, Y.; Cha, J. J.; Hong, S. S.; Cui, Y. Hollow Carbon Nanofiber-Encapsulated Sulfur Cathodes for High Specific Capacity Rechargeable Lithium Batteries. *Nano Lett.* **2011**, *11*, 4462–4467.
- (11) Chen, R.; Zhao, T.; Lu, J.; Wu, F.; Li, L.; Chen, J.; Tan, G.; Ye, Y.; Amine, K. Graphene-Based Three-Dimensional Hierarchical Sandwich-type Architecture for High-Performance Li/S Batteries. *Nano Lett.* **2013**, *13*, 4642–4649.
- (12) Xiao, L. F.; Cao, Y. L.; Xiao, J.; Schwenzer, B.; Engelhard, M. H.; Saraf, L. V.; Nie, Z. M.; Exarhos, G. J.; Liu, J. A Soft Approach To Encapsulate Sulfur: Polyaniline Nanotubes for Lithium–Sulfur Batteries with Long Cycle Life. *Adv. Mater.* **2012**, *24*, 1176–1181.
- (13) Wu, F.; Chen, J.; Chen, R.; Wu, S.; Li, L.; Chen, S.; Zhao, T. Sulfur/Polythiophene with a Core/Shell Structure: Synthesis and Electrochemical Properties of the Cathode for Rechargeable Lithium Batteries. *J. Phys. Chem. C* **2011**, *115*, 6057–6063.
- (14) Wu, F.; Chen, J.; Li, L.; Zhao, T.; Chen, R. Improvement of Rate and Cycle Performance by Rapid Polyaniline Coating of a MWCNT/Sulfur Cathode. *J. Phys. Chem. C* **2011**, *115*, 24411–24417.
- (15) Mikhaylik, Y. V.; Akridge, J. R. Polysulfide Shuttle Study in the Li/S Battery System. *J. Electrochem. Soc.* **2004**, *151*, A1969–A1976.
- (16) Suo, L.; Hu, Y. S.; Li, H.; Armand, M.; Chen, L. A New Class of Solvent-in-Salt Electrolyte for High-Energy Rechargeable Metallic Lithium Batteries. *Nat. Commun.* **2013**, *4*, 1481.
- (17) Lin, Z.; Liu, Z.; Dudney, N. J.; Liang, C. Lithium Superionic Sulfide Cathode for All-Solid Lithium–Sulfur Batteries. *ACS Nano* **2013**, *7*, 2829–2833.
- (18) Aurbach, D.; Pollak, E.; Elazari, R.; Salitra, G.; Kelley, C. S.; Affinito, J. On the Surface Chemical Aspects of Very High Energy Density, Rechargeable Li–Sulfur Batteries. *J. Electrochem. Soc.* **2009**, *156*, A694–A702.
- (19) Xiong, S. Z.; Xie, K.; Diao, Y.; Hong, X. B. Properties of Surface Film on Lithium Anode with LiNO<sub>3</sub> as Lithium Salt in Electrolyte Solution for Lithium–Sulfur Batteries. *Electrochim. Acta* **2012**, *83*, 78–86.
- (20) Zhang, S. S. Role of LiNO<sub>3</sub> in Rechargeable Lithium/Sulfur Battery. *Electrochim. Acta* **2012**, *70*, 344–348.
- (21) Zhang, S. S. Effect of Discharge Cutoff Voltage on Reversibility of Lithium/Sulfur Batteries with LiNO<sub>3</sub>-Contained Electrolyte. *J. Electrochem. Soc.* **2012**, *159*, A920–A923.
- (22) Lin, Z.; Liu, Z.; Fu, W.; Dudney, N. J.; Liang, C. Phosphorous Pentasulfide as a Novel Additive for High-Performance Lithium–Sulfur Batteries. *Adv. Funct. Mater.* **2013**, *23*, 1064–1069.
- (23) Xiong, S.; Kai, X.; Hong, X.; Diao, Y. Effect of LiBOB as Additive on Electrochemical Properties of Lithium–Sulfur Batteries. *Ionics* **2011**, *18*, 249–254.
- (24) Zhang, S. S. An Unique Lithium Salt for the Improved Electrolyte of Li-ion Battery. *Electrochem. Commun.* **2006**, *8*, 1423–1428.
- (25) Zhang, S. S. Electrochemical Study of the Formation of a Solid Electrolyte Interface on Graphite in a LiBc<sub>2</sub>O<sub>4</sub>F<sub>2</sub>-Based Electrolyte. *J. Power Sources* **2007**, *163*, 713–718.
- (26) Zhou, H.; Liu, F.; Li, J. Preparation, Thermal Stability, and Electrochemical Properties of LiODFB. *J. Mater. Sci. Technol.* **2012**, *28*, 723–727.
- (27) Morzilli, S.; Bonino, F.; Scrosati, B. Characteristics of the Lithium Electrode in Organic and Polymeric Electrolytes. *Electrochim. Acta* **1987**, *32*, 961–964.
- (28) Zhang, S. S.; Xu, K.; Jow, T. R. EIS Study on the Formation of Solid Electrolyte Interface in Li-Ion Battery. *Electrochim. Acta* **2006**, *51*, 1636–1640.
- (29) Garreau, M. Cyclability of the Lithium Electrode. *J. Power Sources* **1987**, *20*, 9–17.
- (30) Thevenin, J. G.; Muller, R. H. Impedance of Lithium Electrodes in a Propylene Carbonate Electrolyte. *J. Electrochem. Soc.* **1987**, *134*, 273–280.

(31) Mikhaylik, Y. V.; Kovalev, I.; Schock, R.; Kumaresan, K.; Xu, J.; Affinito, J. High Energy Rechargeable Li–S Cells for EV Application: Status, Remaining Problems, and Solutions. *ECS Trans.* **2010**, *25*, 23–34.

(32) Zhang, S. S. Liquid Electrolyte Lithium/Sulfur Battery: Fundamental Chemistry, Problems, and Solutions. *J. Power Sources* **2013**, *231*, 153–162.

(33) Azimi, N.; Weng, W.; Takoudis, C.; Zhang, Z. Improved Performance of Lithium–Sulfur Battery with Fluorinated Electrolyte. *Electrochem. Commun.* **2013**, *37*, 96–99.

(34) Weng, W.; Pol, V. G.; Amine, K. Ultrasound-Assisted Design of Sulfur/Carbon Cathodes with Partially Fluorinated Ether Electrolytes for Highly Efficient Li/S Batteries. *Adv. Mater.* **2013**, *25*, 1608–1615.

(35) Gordin, M. L.; Dai, F.; Chen, S.; Xu, T.; Song, J.; Tang, D.; Azimi, N.; Zhang, Z.; Wang, D. bis(2,2,2-Trifluoroethyl) Ether as an Electrolyte Co-Solvent for Mitigating Self-Discharge in Lithium–Sulfur Batteries. *ACS Appl. Mater. Interfaces* **2014**, *6*, 8006–8010.

(36) Kanamura, K.; Tamura, H.; Shiraiishi, S.; Takehara, Z. XPS Analysis of Lithium Surfaces Following Immersion in Various Solvents Containing LiBF<sub>4</sub>. *J. Electrochem. Soc.* **1995**, *142*, 340–347.

(37) Zhang, S. S. A Review on Electrolyte Additives for Lithium-Ion Batteries. *J. Power Sources* **2006**, *162*, 1379–1394.

(38) Zhu, Y.; Li, Y.; Bettge, M.; Abraham, D. P. Electrolyte Additive Combinations that Enhance Performance of High-Capacity Li<sub>1.2</sub>Ni<sub>0.15</sub>Mn<sub>0.55</sub>Co<sub>0.1</sub>O<sub>2</sub>-Graphite Cells. *Electrochim. Acta* **2013**, *110*, 191–199.

(39) Shkrob, I. A.; Zhu, Y.; Marin, T. W.; Abraham, D. P. Mechanistic Insight into the Protective Action of Bis(oxalato)borate and Difluoro(oxalato)borate Anions in Li-Ion Batteries. *J. Phys. Chem. C* **2013**, *117*, 23750–23756.